Published in final edited form as:
Am J Physiol Renal Physiol. 2008 May ; 294(5): F1109–F1115. doi:10.1152/ajprenal.00620.2007.

Calcium oxalate crystal deposition in kidneys of hypercalciuric mice with disrupted type IIa sodium-phosphate cotransporter

Saeed R. Khan and **Patricia A. Glenton**
Department of Pathology, Immunology, and Laboratory Medicine, College of Medicine, University of Florida, Gainesville, Florida

Abstract

The most common theories about the pathogenesis of idiopathic kidney stones consider precipitation of calcium phosphate (CaP) within the kidneys critical for the development of the disease. We decided to test the hypothesis that a CaP substrate can promote the deposition of calcium oxalate (CaOx) in the kidneys. Experimental hyperoxaluria was induced by feeding glyoxylate to male mice with knockout (KO) of NaP_i IIa (Npt2a), a sodium-phosphate cotransporter. Npt2a KO mice are hypercalciuric and produce CaP deposits in their renal tubules. Experimental hyperoxaluria led to CaOx crystalluria in both the hypercalciuric KO mice and the normocalciuric control B6 mice. Only the KO mice produced CaOx crystal deposits in their kidneys, but the CaOx crystals deposited separately from the CaP deposits. Perhaps CaP deposits were not available for a CaOx overgrowth. These results also validate earlier animal model observations that showed that CaP substrate is not required for renal deposition of CaOx and that other factors, such as local supersaturation, may be involved. The absence of CaOx deposition in the B6 mice despite extreme hyperoxaluria also signifies the importance of both calcium and oxalate in the development of CaOx nephrolithiasis.

Keywords

hypercalciuria; hyperoxaluria; Randall's plaque; Npt2a knockout mice

Human urinary stones generally contain more than one type of crystal, and there is a tendency for certain crystals to occur together (23). Crystals of calcium oxalate (CaOx) and calcium phosphate (CaP) are the two most common components of urinary stones, and CaOx-CaP combination is found in approximately two-thirds of all idiopathic urinary stones. CaOx and CaP are also the two most common crystals in human urine, with mixed CaOx-CaP crystalluria being more common in stone formers than normal subjects (27). In vitro studies have shown CaP to be a good substrate for nucleation of CaOx in a metastable solution of CaOx (17, 18).

Two of the most common theories about the pathogenesis of idiopathic kidney stones consider precipitation of CaP within the kidneys critical for the development of the disease. According to one theory, urinary conditions in the loop of Henle favor crystallization of CaP (26). These CaP crystals then move with the urine to the collecting ducts, where they promote heterogeneous nucleation of CaOx. Alternatively, CaP crystals form in the collecting ducts and promote crystallization of CaOx (6). According to the other theory, CaP precipitates as apatite in the basement membrane of the loop of Henle and from there

Address for reprint requests and other correspondence: S. R. Khan, Box 100275, Gainesville, FL (khan@pathology.ufl.edu)..

extends outward through the renal interstitium to just under the papillary surface urothelium (7, 21) and promotes the formation of CaOx stones on the papillary surface.

To test the hypothesis that renal deposits of CaP act as a substrate for the deposition of CaOx in the kidneys, we induced hyperoxaluria in mice with knockout (KO) of NaP_i IIa (Npt2a), a sodium-phosphate cotransporter. These mice have been shown to develop intratubular CaP deposits (1, 4, 26). We hypothesized that Npt2a KO mice, when made moderately hyperoxaluric, will produce CaOx crystals in their kidneys and that CaOx will deposit on preformed CaP crystals.

MATERIALS AND METHODS

Mice with disrupted Npt2a cotransporter gene ($Npt2a^{-/-}$) were created by targeted mutagenesis (1). $Npt2a^{-/-}$ mice are viable and fertile, with normal gross appearance and behavior. They exhibit increased urinary excretion of P_i, ~80% decrease in renal brush-border membrane Na-P_i cotransport, and hypophosphatemia, which leads to increased serum 1,25(OH)2D levels, overexpression of intestinal calcium channels, increased intestinal calcium hyperabsorption, and development of hypercalcemia and hypercalciuria (1, 25). $Npt2a^{-/-}$ mice develop intratubular deposits of apatitic CaP (4). Deposits are present in newborn, weanling, and adult mice.

An initial experiment was performed to determine the sites and extent of CaP deposition in the kidneys of normal KO mice. Animal studies were approved by the University of Florida Institutional Animal Care and Use Committee. Kidneys of male and female KO mice 14 days and 2, 4, 6, and 11 mo of age were examined with light microscopic (LM) techniques. Two to four male mice were killed for each age group. Four 5-day-old mice were also examined without determination of their sex.

Four- to six-month-old male B6 wild-type (WT) and Npt2a KO mice weighing 18–30 g were housed in separate cages and were allowed to adjust to their environment for 3 days. Control mice were given regular powdered sterile rodent chow moistened with water and formed into small balls. Treated mice received the chow mixed with 1.5% or 3% glyoxylate (Gox). Food and water consumption as well as mouse weight were monitored regularly. A drop of urine was examined daily to check for the presence of crystals. Mice were housed in mouse metabolic cages for urine collection. Twenty-four-hour urine samples were collected on *days 0*, *3*, *7*, *14*, *21*, and *28*, and their pH was measured. Urine was analyzed for calcium and oxalate. Five mice from each group were killed on *days 14* and *28* with carbon dioxide.

Methods are described in detail in our earlier publications (13, 14). Kidneys were removed, decapsulated, and cut in half. One half was placed in buffered formalin and processed for LM investigation. The other half was placed in a glutaraldehyde-formaldehyde mixture for electron microscopic studies. Bladder contents were removed, put on a nucleopore filter, dried, and examined by scanning electron microscope. Paraffin-embedded sections were examined by light microscope after hematoxylin-eosin staining with and without the use of polarizing optics. Crystal distribution within the kidneys was determined by counting crystal deposits in von Kossa-stained sections with a semiquantitative scoring system in which all crystal deposits visible at ×20 magnification were counted.

RESULTS

Table 1 provides information about distribution of CaP crystal deposits in kidneys of Npt2a KO mice of different ages ranging from newborn to weanling to adult. Crystals were seen in the cortex, medulla, and papilla. The majority of crystals, however, were seen in the renal cortex and outer medulla. Five- to fourteen-day-old mice had the largest number of renal

crystal deposits (Fig. 1*A*). After 4 mo, the number of crystal deposits declined (Fig. 1*B*). This decline was most noticeable in the number of the cortical deposits, which showed a precipitous drop. Crystals appeared limited to the distal tubules and collecting ducts and were not seen in the proximal tubules.

In kidneys of 5-day-old mice crystal deposits were mostly luminal (Fig. 2*A*), often completely filling the tubules, which resulted in flattening of the lining epithelial cells. In many cases crystals completely obliterated the tubules, and surrounding epithelium could not be seen. The kidneys of rats of all ages investigated, from 5 days to 13 mo of age, also contained interstitial crystal deposits (Figs. 2–4). Some definitely appeared interstitial (Fig. 2, *B* and *C*; Fig. 3, *A* and *B*), while others appeared as though they grew too large to be confined to the tubules (Fig. 4) and thus came to rest finally in the renal interstitium. Crystals shown in Fig. 3 may also have started in the nephron, which atrophied after becoming completely filled with CaP crystals. By 6 mo. most crystal deposits appeared located in the renal interstitium. Crystal deposits themselves were von Kossa positive (Figs. 1–4) and often showed growth ring-like internal substructure (Fig. 3, *B* and *C*).

Scanning electron microscopic imaging showed CaP crystal deposits as a solid mass filling the inside of the tubule and taking its shape (Figs. 2*B* and 5*A*). The outer surface of the deposits appeared rough and nodular (Fig. 5*B*), while the interior of the deposits (Fig. 5*C*), exposed by fracturing, appeared amorphous and consisted of distinct central and peripheral areas, the latter being more solid. Elemental analysis by energy-dispersive spectroscopy demonstrated that the two areas had Ca and P_i in different proportions (Fig. 5, *D* and *E*). Crystals in the outer area had a higher Ca-to-P_i ratio, while in the center there appeared to be higher P_i-to-Ca ratio. An earlier study of CaP deposits in Npt2a$^{-/-}$ mice analyzed the crystals with high Ca-to-P_i ratio by selected area electron diffraction and identified them as apatite.

Npt2a KO mice receiving 3% Gox became lethargic by *day 14* and were killed. Mice that received 1.5% Gox, B6 as well as KO, stayed alive for the duration of the study, i.e., 28 days. Both experimental and control B6 mice as well as control KO mice appeared normal, bright, alert, and responsive. However, experimental KO mice that consumed Gox-containing food appeared lethargic.

Consumption of Gox-containing food by both B6 and KO mice was significantly reduced (results not shown). All mice, however, consumed similar amounts of water (results not shown). The control B6 and KO mice maintained their weight, while both types of experimental mice on Gox lost weight (Fig. 6). There was no significant difference in weight between control B6 and control KO mice at any time during the experimental period. There was, however, a significant reduction in weight of the experimental KO mice compared with the control KO mice.

There was no significant difference in urinary pH between control B6 and control KO mice except on *day 21*, when KO mice showed significant increase in urinary pH (Fig. 7). Experimental mice, B6 as well as KO, generally had lower urinary pH than their respective controls. This difference reached significant levels on *day 21* and slight significance on *day 28*.

As expected, KO mice produced significantly higher amounts of urinary calcium compared with B6 mice (Fig. 8). There was no significant change in urinary calcium excretion between control and experimental B6 mice for the first 2 wk. Thereafter, on *days 21* and *28* of the experiment, urinary calcium of experimental B6 mice was significantly reduced compared with control B6 mice. Urinary calcium excretion by experimental KO mice, however, did not differ significantly from control KO mice. By *day 7*, urinary excretion of

oxalate was increased significantly by the consumption of Gox-laden food (Fig. 9) by both B6 and KO mice. Oxalate remained significantly high in the urine of the experimental B6 mice compared with their B6 controls. On *days 14*, *21*, and *28* urinary oxalate of control and experimental B6 mice was significantly higher than urinary oxalate of experimental KO mice. On the other hand, oxalate excretion started to go down in the urine of the KO mice by *day 14*, and by *day 21* it was significantly lower than the oxalate excretion by KO mice on *day 7*.

The urine of control animals was free of CaOx crystals. Glyoxylate-treated B6 as well as KO mice produced both CaOx monohydrate (COM) and CaOx dihydrate (COD) crystals (Fig. 10). COM appeared as platelike, often as interpenetrant twins, while COD had typical pyramidal morphology (not shown). KO mice had more COM crystals in their urine than B6 mice.

Microscopic analyses of the kidneys showed that B6 mice, both control and experimental, did not produce crystals of CaP or CaOx. Control KO mice showed deposits of CaP, distributed throughout the kidneys, but mostly in the cortex. After 14 days of treatment kidneys of 50% of the KO mice (4/8) contained both CaP and CaOx crystal deposits (Fig. 11) and CaOx deposits were mostly limited to the renal medullary collecting ducts. After 28 days of treatment kidneys of all KO mice contained both type of crystals. However, no direct connection was seen between the CaP and CaOx crystals. These two types of crystals were located separately.

Even though CaOx crystals were seen in both the cortex and the medulla, crystal deposits seen in the cortical tubules appeared larger than those in the medulla and papilla. A closer examination of smaller deposits indicated that CaOx crystals were, at least initially, intraluminal and present in both the collecting ducts and the limbs of the loop of Henle. Crystal deposition was associated with flattening of the surrounding epithelial cells. Some CaOx crystals appeared interstitial. Some were also seen inside the tubular epithelial cells (Fig. 11). CaOx crystal deposits were highly birefringent, and individual crystals had a tabular habit (Fig. 12) aggregated into rosettes, suggesting that most consisted of COM. Elemental analysis by energy-dispersive spectroscopy demonstrated a single major peak for calcium.

DISCUSSION

The results of our study presented here confirm earlier observation of CaP deposition in kidneys of $Npt2^{-/-}$ mice as well as a reduction in the number of renal deposits with age (4). We additionally demonstrate the presence of interstitial CaP deposits, whose number does not appear to change with age. The interstitial crystals were present as early as 5 days. The reduction in number is most likely a result of the disappearance of luminal crystal deposits, as has already been suggested. The kidneys of newborn mice are still growing. Their glomerular filtration rate (GFR) may be slower and tubular luminal diameter smaller, leading to mineral retention. Increased GFR during adulthood may move the urine more rapidly, causing the luminal crystal deposits to be dislodged and excreted in the urine. Interstitial crystal deposits, on the other hand, do not have a similar option. Additional studies are necessary to determine the factors responsible for age-dependent depletion in renal calcification. Further studies are also needed to investigate the origin of interstitial crystals.

This study was performed to test the hypothesis that under hyperoxaluric conditions renal CaP deposits can act as a substrate for CaOx crystallization. Npt2a KO mice are born with CaP crystal deposits in all segments of the renal tubules of both the cortex and medulla (4).

When these mice were made hyperoxaluric, they developed CaOx crystals in their renal tubules but not on the preexisting CaP crystals, indicating that factors other than CaP may be involved. Alternatively, CaP deposits may not be accessible to oxalate for the formation and development of a CaOx overgrowth, CaP deposits totally blocking the tubules or being present in the interstitium. We showed previously (13) that in a rat model of hypercalciuria CaOx crystals did not deposit on CaP crystals. In the rat model of genetic idiopathic hypercalciuria, experimentally induced hyperoxaluria resulted in codeposition of CaOx and CaP in renal pelvis of the hypercalciuric rats (3). In a recent study rats with small bowel resection fed a high-oxalate diet developed extensive CaOx and CaP crystals in the kidneys. It was concluded that CaOx crystals injured the cells, causing local acidification disorders and leading to higher lumen pH and transformation of CaOx to apatite (28).

Even though both CaP and CaOx crystals were seen in all segments of the kidneys of the hyperoxaluric mice, CaP crystals were seen primarily in the cortical distal tubules, while CaOx crystals were generally seen in the medullary collecting ducts. CaOx and CaP crystals deposited in different sections of the renal tubules even in a rat model in which both hypercalciuria and hyperoxaluria were experimentally induced. Results of a number of studies have indicated that CaP supersaturation is reached in earlier sections of the renal tubules, where the urinary pH is high, while that of CaOx is reached in the collecting ducts, where urine is concentrated and urinary pH is low (6, 26). Separate deposition of the two types of crystals in the hyperoxaluric Npt2a KO mice may be a result of the supersaturations for the two salts being reached in different segments of the renal tubules. CaP supersaturation occurs in the proximal tubule and loop, while CaOx supersaturation occurs in the collecting ducts. Since pelvic urine is also supersaturated with respect to CaOx, there is a distinct possibility of its crystallization in renal pelvis, regardless of the presence or absence of a plaque. It is, however, possible that the presence of subepithelial plaque makes it easier for crystal adherence to papillary surface, as originally suggested by Randall (21).

It has often been debated whether urinary oxalate or calcium is the most important risk factor in the formation of CaOx kidney stones. The results presented here indicate that in vivo, with other conditions being equal, both calcium and oxalate are equally important for stone formation. Hyperoxaluria alone did not produce renal CaOx crystal deposits in the control mice. Only the Npt2a KO mice with both hypercalciuria and hyperoxaluria developed CaOx crystal deposits. Even though most rats with experimentally induced hyperoxaluria develop CaOx renal deposits, mouse models of hyperoxaluria produce only a few CaOx crystals in their kidneys. Alanine glyoxylate aminotransferase KO mice develop severe hyperoxaluria but develop only a few CaOx crystal deposits in their kidneys (22). Mice lacking anion transporter Slc26a6 also develop severe hyperoxaluria (10, 12), but only those with high urinary calcium excretion develop CaOx crystal deposits, indicating the importance of both calcium and oxalate in the development of CaOx stones.

High urinary pH favors CaP crystallization, while CaOx crystallization is favored at lower, more neutral pH (5, 6, 26). In our studies described here, hyperoxaluria did not produce a significant change in urinary pH of the B6 control mice and was associated with the absence of CaOx crystallization in the kidneys. On the other hand, urinary pH of the hyperoxaluric KO mice dropped and was associated with renal CaOx crystal deposition. We saw a similar effect of pH on CaOx crystal deposition on a foreign body introduced into the urinary bladder of rats, with hyperoxaluria induced by the administration of ethylene glycol (15, 16).

Can hypercalciuria alone lead to interstitial CaP deposition? A series of events involving an increase in interstitial calcium around the thin limbs of the loop and an increase in the pH of the medullary interstitium have been proposed (2, 11). However, the contribution of such events to interstitial CaP deposition has yet to be tested. None of the existing animal models

of hypercalciuria, genetic or otherwise, has shown such interstitial crystal deposition (19). Even urinary CaP deposits are seen in only two of more than a dozen animal models of monogenic hypercalciuria, Npt2a KO and caveolin-1 KO mice, and only Npt2a KO mice develop deposits in their kidneys. Caveolin-1 KO mice produce bladder stones. A recent study of calcification in mice deficient in osteopontin (OPN) and/or Tamm-Horsfall protein (THP) showed that 10% of the mice lacking OPN and 14.3% of the mice lacking THP spontaneously form interstitial deposits of CaP within the renal papillae (20). Experimental induction of hypercalciuria in rats by administration of vitamin D also resulted in the intratubular deposition of CaP (24). Similarly, weanling rats given AIN-76 diet became hypercalciuric and produced intratubular concretions of CaP (13). Rats selectively bred for hypercalciuria also did not produce CaP crystals in the renal interstitium (3).

Overall, our studies confirm the results of earlier rat and mouse model studies demonstrating that hypercalciuria-induced CaP crystallization mostly occurs in the renal tubules. Lesions seen in the KO mice may be similar to what might be seen in patients with brushite stones. In that respect, hypercalciuria is similar to hyperoxaluria, cystinuria, and uricosuria, which also lead to the intratubular deposition of CaOx, cystine, and uric acid crystals, respectively (7–9). Interestingly, CaOx crystals did not grow on preexisting intratubular or interstitial CaP deposits, suggesting that such deposits were not available for an overgrowth. The results also indicate that, at least in mice, hyperoxaluria is not sufficient for intratubular crystallization of CaOx. Hypercalciuria is also required. Thus this mouse model is, to some extent, similar to idiopathic CaOx nephrolithiasis in humans, where CaP deposits are seen in the medullary interstitium and both hyperoxaluria and hypercalciuria are considered essential for stone formation. It should, however, be recognized that whereas idiopathic CaOx stones probably arise over months to years, the pathology seen in the KO mice took only weeks to develop.

Acknowledgments

GRANTS

This work was supported by National Institute of Diabetes and Digestive and Kidney Diseases Grant RO1-DK-065658 and the University of Florida Center for the Study of Lithiasis.

REFERENCES

1. Beck L, Karaplis AC, Amizuka N, Hewson AS, Ozawa H, Tenenhouse HS. Targeted inactivation of Npt2 in mice leads to severe renal phosphate wasting, hypercalciuria, and skeletal abnormalities. Proc Natl Acad Sci USA. 1998; 95:5372–5377. [PubMed: 9560283]
2. Bushinsky DA. Nephrolithiasis: site of initial solid phase. J Clin Invest. 2003; 111:602–605. [PubMed: 12618514]
3. Bushinsky DA, Asplin JR, Grynpas MD, Evan AP, Parker WR, Alexander KM, Coe FL. Calcium oxalate stone formation in genetic hypercalciuric stone-forming rats. Kidney Int. 2002; 61:975–987. [PubMed: 11849452]
4. Chau H, El-Maadawy S, McKee MD, Tenenhouse HS. Renal calcification in mice homozygous for the disrupted type IIa Na/Pi cotransporter gene Npt2. J Bone Miner Res. 2003; 18:644–657. [PubMed: 12674325]
5. Coe FL, Evan A, Worcester E. Kidney stone disease. J Clin Invest. 2005; 115:2598–2608. [PubMed: 16200192]
6. Evan AP, Bledsoe SB, Smith SB, Bushinsky DA. Calcium oxalate crystal localization and osteopontin immunostaining in genetic hypercalciuric stone-forming rats. Kidney Int. 2004; 65:154–161. [PubMed: 14675046]

7. Evan AP, Lingeman JE, Coe FL, Parks JH, Bledsoe SB, Shao Y, Sommer AJ, Paterson RF, Kuo RL, Grynpas M. Randall's plaque of patients with nephrolithiasis begins in basement membranes of thin loops of Henle. J Clin Invest. 2003; 111:607–616. [PubMed: 12618515]
8. Evan A, Lingeman J, Coe FL, Worcester E. Randall's plaque: pathogenesis and role in calcium oxalate nephrolithiasis. Kidney Int. 2006; 69:1313–1318. [PubMed: 16614720]
9. Evan AP, Lingeman J, Coe F, Shao Y, Miller N, Matlaga B, Phillips C, Sommer A, Worcester E. Renal histopathology of stone-forming patients with distal tubular acidosis. Kidney Int. 2007; 71:795–901. [PubMed: 17264873]
10. Freel RW, Hatch M, Green M, Soleimani M. Ileal oxalate absorption and urinary oxalate excretion are enhanced in Slc26a6 null mice. Am J Physiol Gastrointest Liver Physiol. 2006; 290:G719–G728. [PubMed: 16373425]
11. Halperin ML, Dhadi SC, Kamel KS. Physiology of acid-base balance: links with kidney stone prevention. Semin Nephrol. 2006; 26:441–446. [PubMed: 17275581]
12. Jiang Z, Asplin JR, Evan AP, Rajendran VM, Velazquez H, Nottoli TP, Binder HJ, Aronson PS. Calcium oxalate urolithiasis in mice lacking anion transporter Slc26a6. Nat Genet. 2006; 38:474–478. [PubMed: 16532010]
13. Khan SR, Glenton PA. Deposition of calcium phosphate and calcium oxalate crystals in the kidneys. J Urol. 1995; 153:811–817. [PubMed: 7861545]
14. Khan SR, Glenton PA, Byer KJ. Modeling of hyperoxaluric calcium oxalate nephrolithiasis: experimental induction of hyperoxaluria by hydroxy-l-proline. Kidney Int. 2006; 70:914–923. [PubMed: 16850024]
15. Khan SR, Hackett RL. Urolithogenesis of mixed foreign body stones. J Urol. 1987; 138:1321–1328. [PubMed: 3312647]
16. Khan SR, Hackett RL. Role of organic matrix in urinary stone formation: an ultrastructural study of crystal matrix interface of calcium oxalate monohydrate stones. J Urol. 1993; 150:239–245. [PubMed: 8510264]
17. Koutsoukos PG, Sheehan ME, Nancollas GH. Epitaxial considerations in stone formations. Invest Urol. 1981; 18:358–364. [PubMed: 7203960]
18. Meyer JL, Bergert JH, Smith LH. Epitaxial relationships in urolithiasis: the calcium oxalate-hydroxyapatite system. Clin Sci Mol Med. 1975; 46:369–374. [PubMed: 1192695]
19. Moe OW, Bonny O. Genetic hypercalciuria. J Am Soc Nephrol. 2005; 16:729–745. [PubMed: 15689405]
20. Mo L, Liaw L, Evan AP, Sommer AJ, Lieske JC, Wu XR. Renal calcinosis and stone formation in mice lacking osteopontin, Tamm-Horsfall protein, or both. Am J Physiol Renal Physiol. 2007; 293:F1935–F1943. [PubMed: 17898038]
21. Randall A. The etiology of primary renal calculus. Int Abst Surg. 1940; 71:209–240.
22. Salido EC, Li XM, Wang X, Santana A, Roy-Chowdhury N, Torres A, Shapiro LJ, Roy-Chowdhury J. Alanine-glyoxylate aminotransferasedeficient mice, a model for primary hyperoxaluria that responds to adenoviral gene transfer. Proc Natl Acad Sci USA. 2006; 103:18249–18254. [PubMed: 17110443]
23. Schneider, HJ. Epidemiology of urolithiasis.. In: Schneider, HJ., editor. Urolithiasis: Etiology, Diagnosis. Springer; Berlin: 1985. p. 138
24. Strohmaier WL, Seeger RD, Osswald H, Bichler KH. Reduction of vitamin D induced stone formation by calcium antagonist. Urol Res. 1994; 22:301–303. [PubMed: 7879315]
25. Tenenhouse HS. Regulation of phosphorus homeostasis by the type IIa Na/phosphate cotransporter. Annu Rev Nutr. 2005; 25:197–214. [PubMed: 16011465]
26. Tiselius HG. Estimated levels of supersaturation with calcium phosphate and calcium oxalate in the distal tubule. Urol Res. 1997; 25:153–159. [PubMed: 9144885]
27. Werness PG, Wilson JWL, Smith LH. Crystalluria. J Cryst Growth. 1981; 53:166–173.
28. Worcester E, Evan A, Bledsoe S, Lyon M, Chuang M, Orvieto M, Gerber G, Coe F. Pathophysiological correlates of two unique renal tubule lesions in rats with intestinal resection. Am J Physiol Renal Physiol. 2006; 291:F1061–F1069. [PubMed: 17028259]

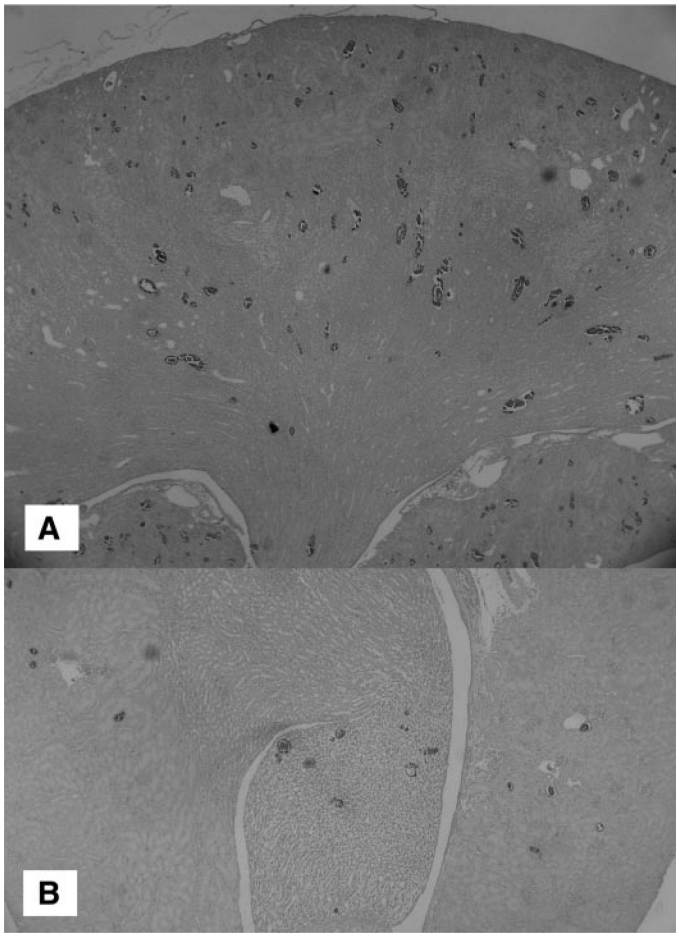

Fig. 1.

Nephrolithiasis in mice with disrupted type IIa sodium-phosphate cotransporter (Npt2a). *A*: von Kossa-stained paraffin section of a kidney from a 5-day-old male knockout (KO) mouse. The von Kossa method specifically detects calcium deposits. Section shows von Kossa-positive calcium phosphate (CaP) deposits throughout the kidney. Most deposits are seen in the renal cortex and outer medulla. *B*: von Kossa-stained paraffin section of a kidney from a 4-mo-old male KO mouse showing the presence of a very few crystal deposits. Original magnification ×1.2.

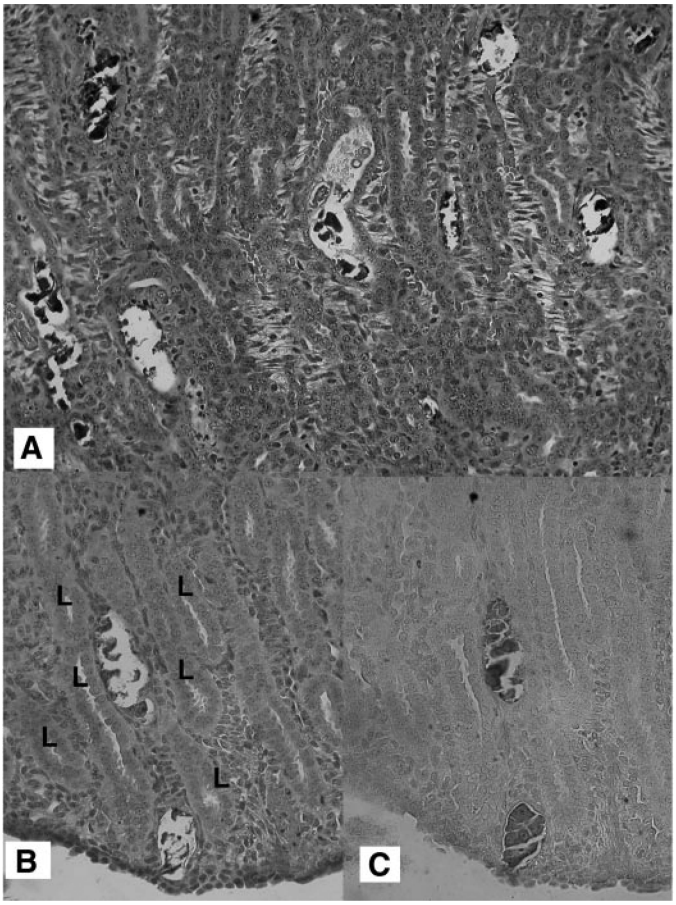

Fig. 2.

A: hematoxylin and eosin (H & E)-stained paraffin section of a kidney from a 5-day-old KO mouse showing CaP deposits in outer medulla. Crystals are mostly intraluminal. *B*: renal papilla of the same kidney showing patent collecting ducts (L) and CaP deposits in the renal interstitium. *C*: same deposit after von Kossa staining. Original magnification ×20.

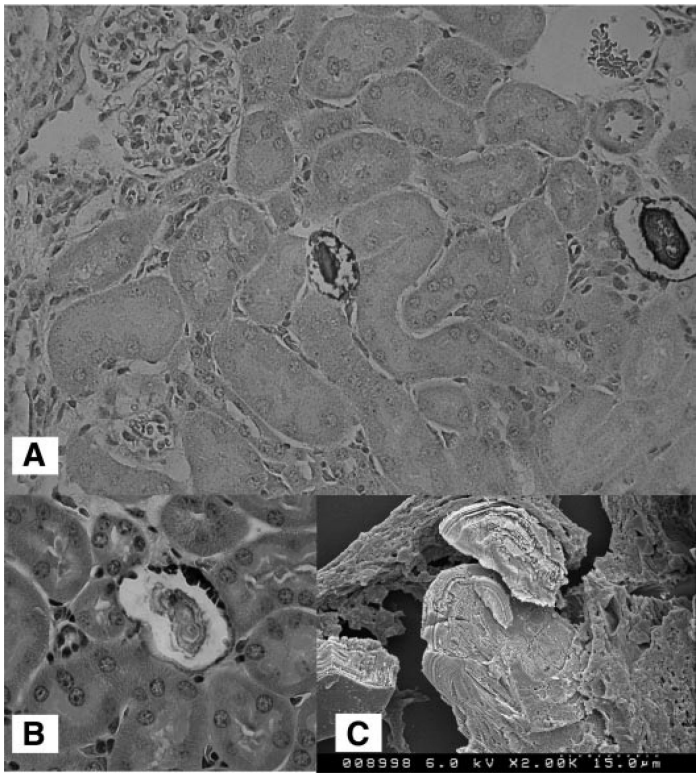

Fig. 3.
A: von Kossa-stained paraffin section of a kidney from a 2-mo-old KO mouse showing interstitial deposits in the renal cortex. Renal tubules are completely devoid of any crystals. Original magnification ×20. *B*: higher magnification showing ringlike substructure in the crystal deposit. Original magnification ×40. *C*: scanning electronic microscopic (SEM) image of a similar CaP crystal deposit showing internal concentric laminations.

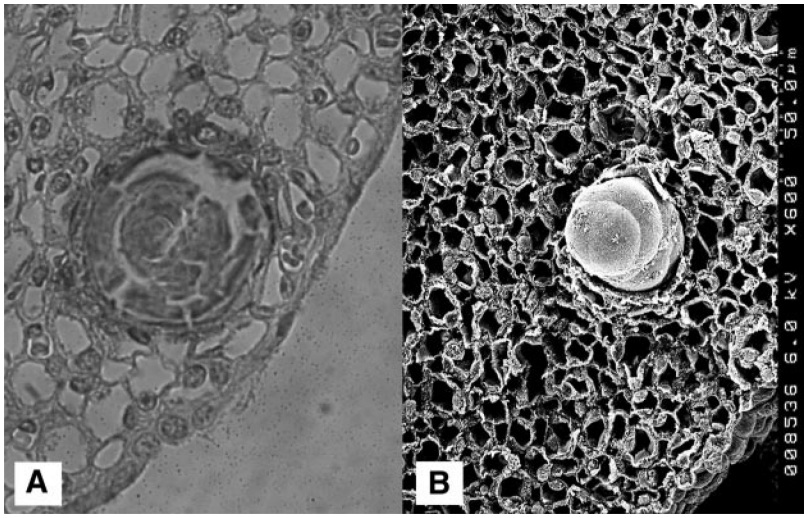

Fig. 4.

A: von Kossa-stained paraffin section of a kidney from a 2-mo-old KO mouse showing a large CaP deposit in the inner medullary portion of the renal papilla. Original magnification ×20. *B*: SEM image of a similar deposit. The size and shape of crystal deposits indicates that they started in the renal tubules, grew beyond the tubular dimension, and secondarily came to lie in the renal interstitium.

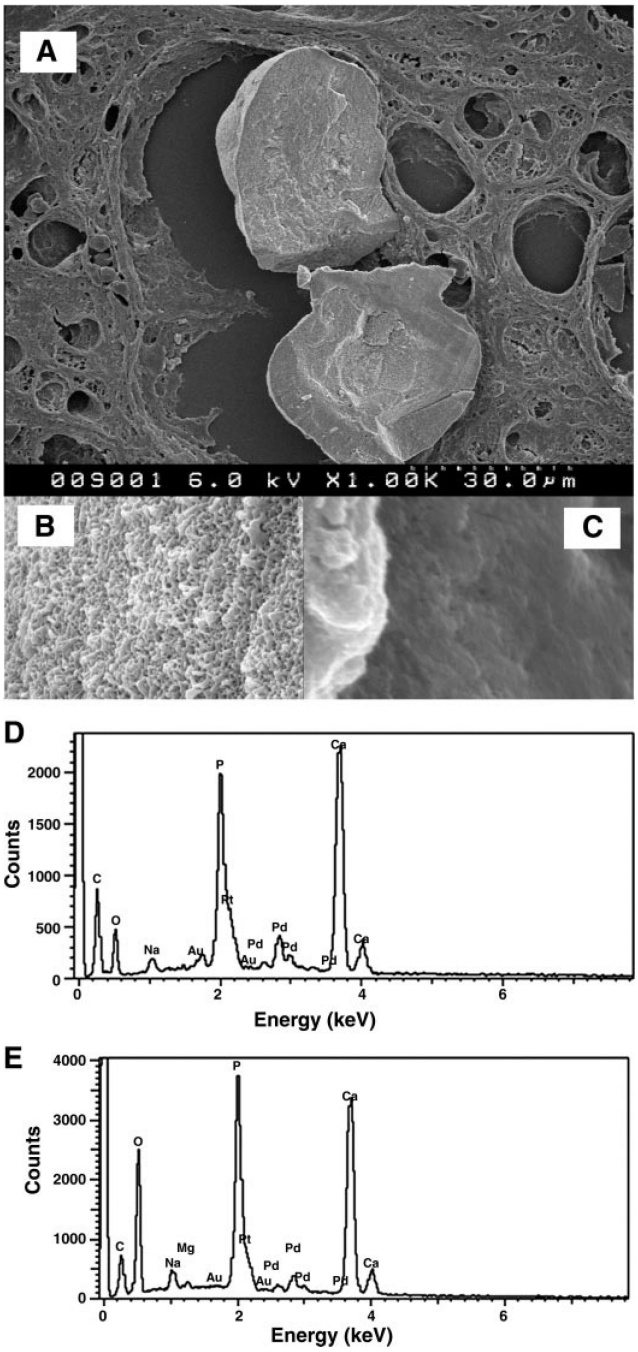

Fig. 5.

SEM analyses of a renal CaP crystal deposit. *A*: surface of a fractured CaP deposit. *B*: high magnification of the surface showing its rough appearance. *C*: high magnification of the central part of the CaP deposit showing amorphous nature. *D*: energy-dispersive X-ray microanalysis of the peripheral area of the deposit showing major peaks for calcium (Ca) and phosphorus (P). Ca peak is slightly higher than P peak. *E*: energy-dispersive X-ray microanalysis of the central area of the deposit showing major peaks for Ca and P. Here the Ca peak is slightly lower than the P peak.

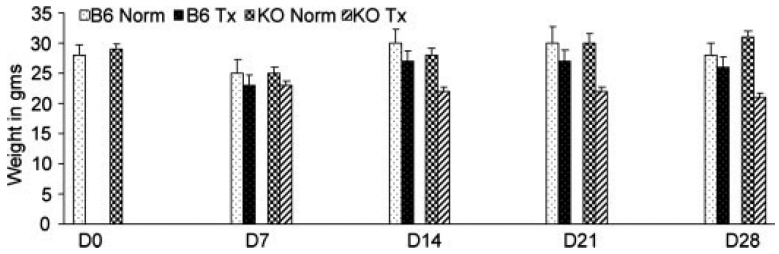

Fig. 6.

Weight change during 28 days of the experiment. Control (Norm) B6 and KO mice maintained their weight, while both types of experimental (Tx) mice who received glyoxylate (Gox) in food lost their weight. There was no significant difference in weight between the normal B6 and KO mice at any time during the experimental period. However, there was a gradual reduction in weight of the experimental KO mice compared with the control KO mice, and experimental mice had significantly reduced weight compared with their controls on *days* (D) *14* ($P < 0.001$), *21* ($P < 0.001$), and *28* ($P < 0.001$).

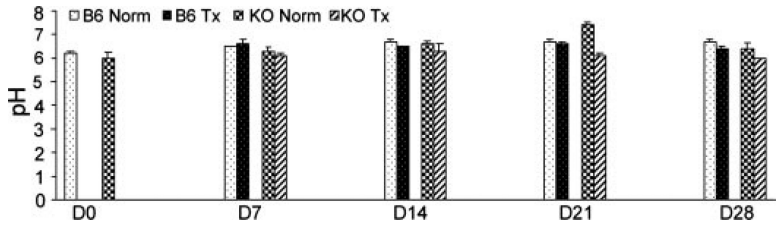

Fig. 7.

Urinary pH. There was no significant difference in urinary pH between control (Norm) B6 and control KO mice except on *day 21*, when KO mice showed significant increase in urinary pH ($P < 0.003$). Experimental (Tx) mice, B6 as well as KO, generally had lower urinary pH than their respective controls. This difference reached significant levels on *day 21* ($P < 0.001$) and slight significance ($P < 0.059$) on *day 28*.

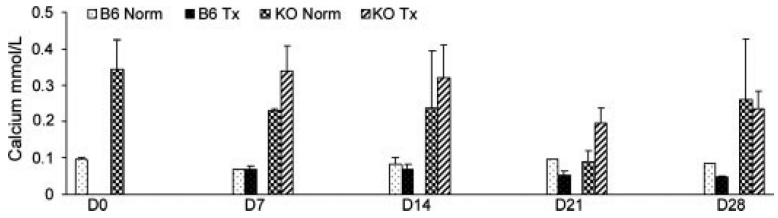

Fig. 8.

Urinary calcium. There was no significant difference in urinary calcium excretion between control (Norm) and experimental (Tx) B6 mice for the first week. However, urinary excretion of calcium by the experimental B6 mice became significantly lower on *days 21* ($P < 0.037$) and *28* ($P < 0.001$). Urinary calcium excretion by the experimental (Tx) KO mice, however, did not differ significantly from the control KO mice.

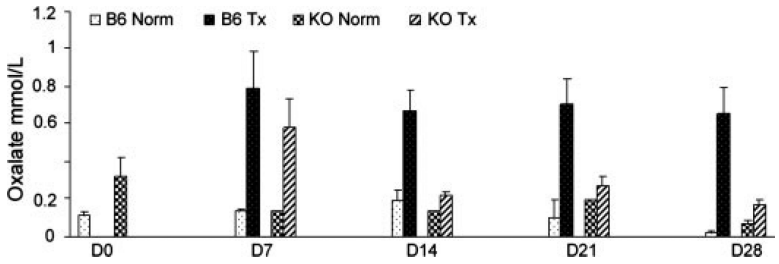

Fig. 9.

Urinary oxalate. By *day 7* of Gox treatment, urinary excretion of oxalate by the experimental (Tx) B6 as well as KO mice increased significantly compared with their respective controls. Oxalate remained significantly high in urine of the experimental B6 mice compared with their B6 controls and on *days 14*, *21*, and *28* compared with the experimental KO mice. On the other hand, oxalate excretion started to go down in the urine of the KO mice by *day 14*, and by *day 21* it was significantly lower than the oxalate excretion by KO mice on *day 7*.

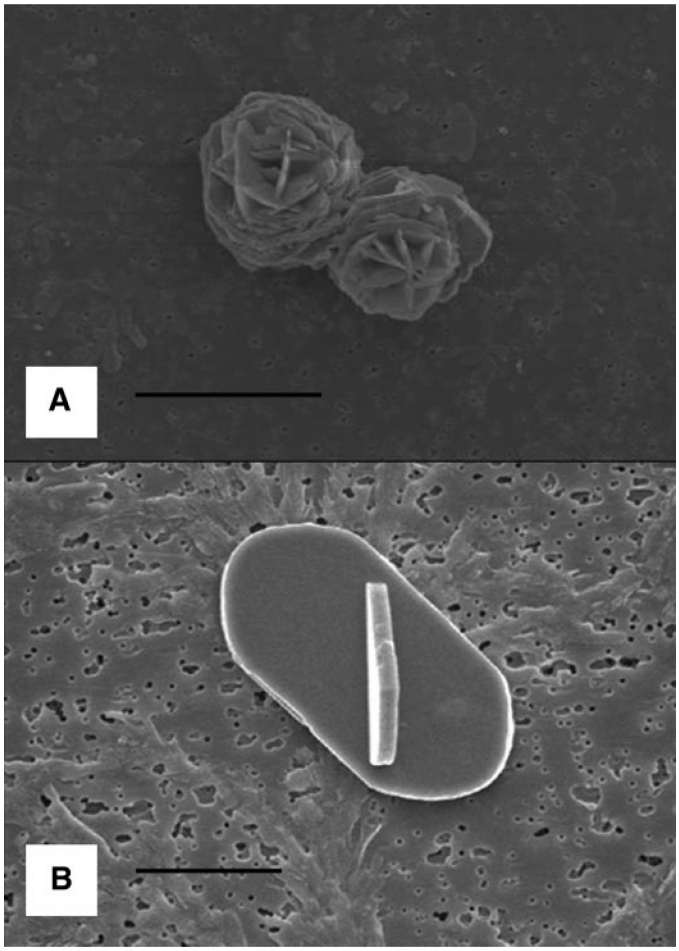

Fig. 10.
SEM images of urinary crystals of mice treated with Gox. *A* and *B*: calcium oxalate (CaOx) monohydrate (COM) crystals, which appeared as interpenetrant twins of platelike crystals. CaOx dehydrate crystals (not shown) appeared as tetragonal bipyramids. Bar, 6 μm.

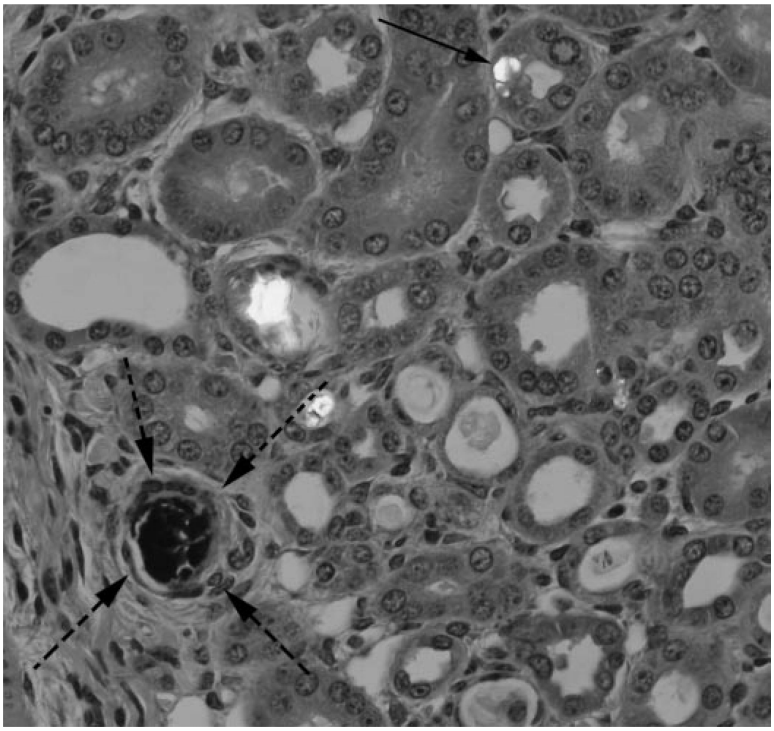

Fig. 11.

H & E-stained paraffin section of a kidney of an experimental KO mouse on *day 14* of Gox treatment showing both birefringent CaOx crystal deposits and dark CaP crystal deposits. Birefringent CaOx crystals are mostly intraluminal. Epithelial cell of a renal tubule also contains an intracellular CaOx crystal (arrow). CaP deposit appears to be surrounded by a ring of inflammatory cells (dashed arrows). Original magnification ×20.

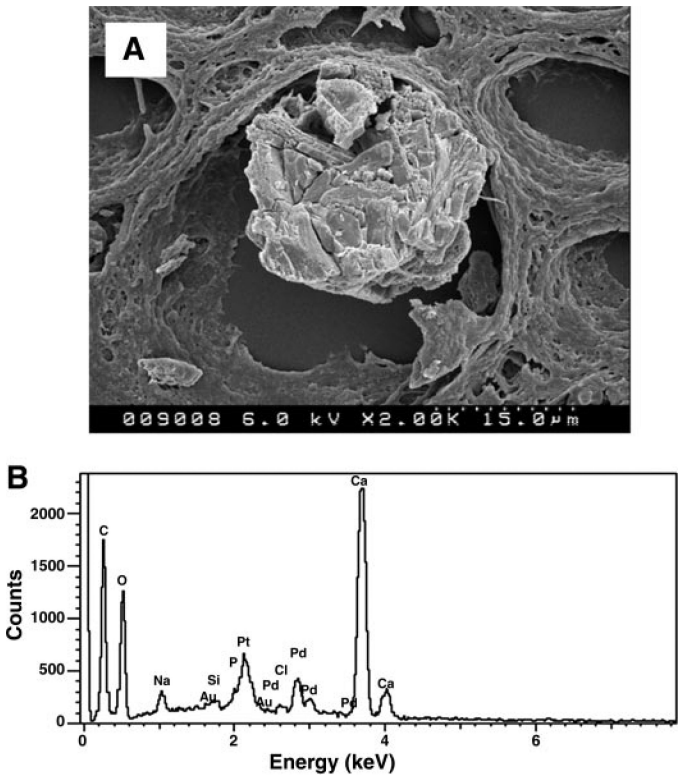

Fig. 12.
SEM analyses of renal CaOx crystal deposit. *A*: deposit shows highly compact aggregate of platelike COM crystals. *B*: energy-dispersive X-ray microanalysis of the deposit shows major peak for calcium.

Table 1

Distribution of calcium phosphate crystals in kidneys of mice of different ages

Age	Cortex	Medulla	Papilla
5 days	+++++	+++	+
2mo	+++	++	+
4mo	+++	++	+
6mo	++	++	+
11 mo	+	+	+
13 mo	+	+	+

von Kossa-stained paraffin sections were examined and crystal deposits counted at 20× magnification. On the basis of that examination, a severity grade was assigned: +, 1–5 deposits; + + , 5–10 deposits; + + + , 10–30 deposits; + + + + + , >30 deposits.